Heliyon 9 (2023) e21030

Contents lists available at ScienceDirect

Heliyon

journal homepage: www.cell.com/heliyon

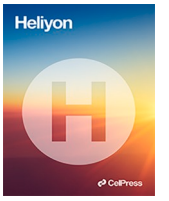

Magnetic layered double hydroxides with carbamazepine for breast cancer treatment

M. Florencia Peralta [a], Silvia N. Mendieta [a,*], I. Romina Scolari [b], M. Verónica Gerbaldo [a], Marcos I. Oliva [c], Germán A. Gil [d], Gladys E. Granero [b], Mónica E. Crivello [a]

[a] *Centro de Investigación y Tecnología Química (CITeQ), UTN-CONICET, Av. Cruz Roja Argentina y Maestro López, Córdoba, 5000, Argentina*
[b] *Unidad de Investigación y Desarrollo en Tecnología Farmacéutica (UNITEFA), UNC-CONICET, Departamento de Ciencias Farmacéuticas, Universidad Nacional de Córdoba, Av. Medina Allende S/N, Córdoba, 5000, Argentina*
[c] *Instituto de Física Enrique Gaviola (IFEG), UNC-CONICET, Facultad de Matemática, Astronomía, Física y Computación, UNC, Av. Medina Allende S/N, Córdoba, 5000, Argentina*
[d] *Centro de Investigaciones en Química Biológica de Córdoba (CIQUIBIC), UNC-CONICET, Av. Haya de la Torre S/N, Córdoba, 5000, Argentina*

ARTICLE INFO

Keywords:
Nanoclay
Carbamazepine
Cancer therapy
Layered double hydroxide
Nanoparticle

ABSTRACT

Current cancer chemotherapy is associated with many side effects and, in some cases, drug resistance, which makes the search for new active molecules and drug delivery strategies imperative. Carbamazepine is an antiepileptic compound that has shown efficacy against breast cancer cell lines. In this study, it was incorporated into layered double hydroxide nanoclays, the percentage of drug loading was increased compared to previous research, and the clays were impregnated with magnetic Fe_3O_4 nanoparticles. The goal of the magnetic Fe_3O_4-impregnation was to direct the nanocomposites to the therapeutic target with an external magnetic field. The nanoclay-carbamazepine composites had a carbamazepine loading of 51 %, and the nanoclay-carbamazepine-nanoparticles had a drug loading of 13 % due to the addition of more ingredients. The structure of the composites was analyzed by X-ray diffraction and Scherrer equation, showing a layered double hydroxide organization with crystal sizes of 9–15 nm; from transmission electron microscopy, the final compounds showed a particle size of 97–158 nm, small enough for systemic circulation. In vibrating sample magnetization studies, the composites showed a superparamagnetic behavior with high magnetic saturation (9–17 emu/gr), which should allow a good material attraction by an external magnetic field located near the tumor. *In vitro* drug release studies were done in Franz cells and measured by UV/Vis spectrophotometry; they showed that carbamazepine release from the nanocomposites responds to the media pH: a good drug release at the lysosome pH and slow release at the blood pH. Finally, the efficacy was tested *in vitro* in MDA-MB-231 breast cancer cells, and the composites showed an enhanced efficacy in comparison with that produced by the free drug (96 % and 62 % of cell inhibition respectively). Carbamazepine administered with magnetic clays as a carrier is a promising treatment for breast cancer, and further studies should be done to measure the arrival time and the efficacy *in vivo*.

* Corresponding author. Maestro López esq. Cruz Roja Argentina, S/N X5016ZAA, Córdoba, Argentina.
E-mail address: smendieta@frc.utn.edu.ar (S.N. Mendieta).

https://doi.org/10.1016/j.heliyon.2023.e21030
Received 17 April 2023; Received in revised form 28 September 2023; Accepted 13 October 2023
Available online 14 October 2023

1. Introduction

Cancer is still one of the most deadly diseases worldwide, with breasts and lungs cancer having the highest incidence rate [1,2]. In chemotherapy, the collateral effects of the drugs are the main problem. Nanotechnology has advanced considerably in the delivery of very toxic drugs, in order to direct them to the therapeutic target and avoid their activity in healthy organs [3].

On the other hand, new molecules are necessary to avoid cancer cell resistance. In this sense, compounds that are approved to treat other diseases are usually tested against different cancer cells. Carbamazepine (CBZ) is an antiepileptic drug with low water solubility that has shown activity against breast cancer [4,5] and human colon adenocarcinoma [6] cell lines. The use of inorganic matrices has been reported to enhance the solubility of many similar molecules [7].

Layered double hydroxides (LDHs) are anionic nanoclays composed of positive layers of metals (M), M^{+2} and M^{+3}, and an aqueous interlayer that encloses anionic molecules. After calcination at 450 °C, LDHs convert into mixed oxides [8], and when in contact with and aqueous environment, due to the so-called "memory effect", they can reconstruct into the original LDHs. In this process, the positive layers can enclose the water molecules and the anions present in the medium. Moreover, it has been previously demonstrated that neutral molecules such as carbamazepine can also be enclosed in the interlayer during the reconstruction [9]. LDHs are attractive in drug delivery since they are biocompatible, penetrate the cell membrane easily, and protect the attached drugs during blood circulation (pH 7.4) by maintaining their structure, while releasing them in the lysosomes of cancer cells (pH 4.8) by disintegration [10, 11]. Ambrogi loaded CBZ in SBA-15 with high drug loading (40 wt%) [12] but these silicates are more expensive than the LDHs. Moreover, Donnadio et al. studied CBZ with $CaCO_3$ as an antiepileptic [13].

On the other hand, magnetic nanoparticles (NP) such as magnetite (Fe_3O_4) are interesting since they can be driven to the therapeutic target by an external magnetic field. Furthermore, below 15 nm, iron NP have superparamagnetic behavior, which implies that they will be left without remanent magnetization after removal of the external magnetic field [3]. Many researchers have studied Fe_3O_4 in structures such as silica, polymer, and vesicles for targeting transport [14]. NP can be coated with citric acid in order to stabilize them, avoiding their agglomeration, and additionally, to give them a charge that will allow the interaction with the positively charged LDHs [15].

The Fe_3O_4 NP – LDH nanocomposites have gained interest in the last years to be used in different fields such as environmental remediation, photocatalysis, and drug delivery because of their flexible properties [8]. However, the evidence of Fe_3O_4 NP – LDH activity as antitumor agents is scarce. Zhao et al. showed that core-shell Fe_3O_4 NP – LDHs loaded with methotrexate and coated with Au NP significantly reduce the viability of lung cancer cells, while the Fe_3O_4 NP alone showed little effect [16]. Komarala et al. developed Fe_3O_4 NP – LDHs loaded with doxorubicin by hydrothermal method and decreased the IC_{50} of the drug in cervical cancer cells, while the composites alone produced no effect [17]. Barkhordari prepared chitosan/LDH/Fe_3O_4 and found that the application of a magnetic field affected the drug release behavior, although less than the pH effect [18].

In this work, LDHs of Mg and Al were prepared by co-precipitation, calcined, and reconstructed for CBZ incorporation. The drug-loaded LDHs were stirred in an aqueous solution with previously synthesized Fe_3O_4 NP. The hydrothermal process produced nanocomposites composed of LDH-CBZ-NP that were characterized by X-ray diffraction, vibrating sample magnetization (VSM), transmittance electron microscopy, drug release, and anticancer activity against breast cancer cells. The Fe_3O_4 NP are magnetic; the impregnation of the LDH-CBZ systems with the NP will allow the drug to be directed more quickly to the therapeutic target by an external magnetic field located near the tumor site. Also, the LDHs should protect the drug during blood circulation (slow down its release at pH 7.4) and release it faster in the lysosomes (pH 4.8). Finally, CBZ activity against breast cancer cells should be maintained or enhanced with the presence of the composites.

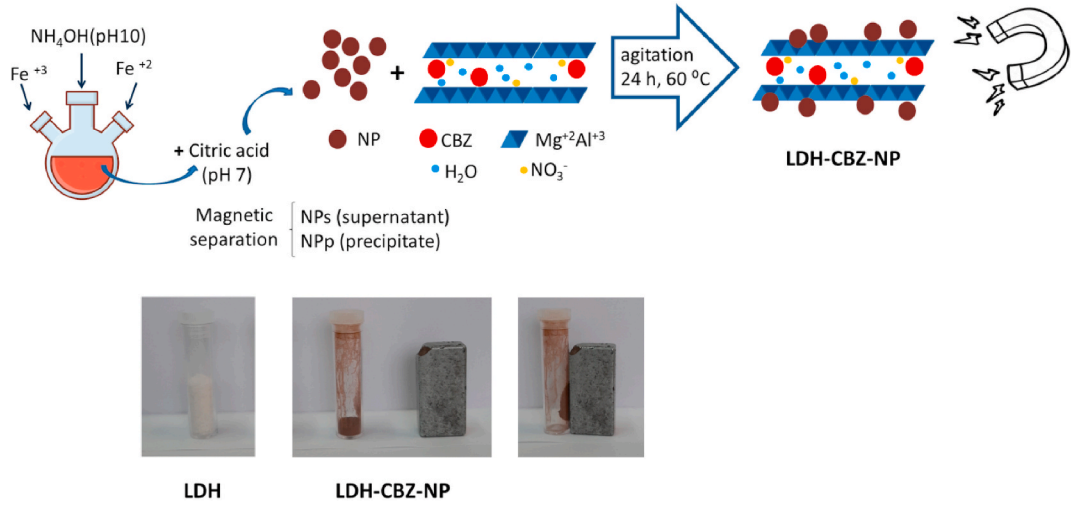

Fig. 1. Scheme of the NP synthesis and LDH-CBZ impregnation, and photographs of the resultant composites. Notice the magnetic attraction of the final material impregnated with NP.

2. Methodology

2.1. Materials

Carbamazepine (USP grade, Parafarm) was purchased from Saporiti, Argentina. Al(NO3)2·9H2O (98 %) was obtained from Sigma Aldrich, St. Louis, USA. Mg(NO3)2·6H2O (98 %) and NaOH (97 %) were provided by Biopack and ethanol (absolute grade) by Sintorgan.

2.2. Synthesis of the composites

Layered double hydroxides were synthesized by co-precipitation from Mg and Al nitrates, as described in Peralta 2021 [9].

NP were synthesized as described in de Sousa 2013 [15] with some modifications (Fig. 1). Briefly, 1.0 g of $FeCl_3{\cdot}4H_2O$ and 0.4 g of $FeCl_2{\cdot}6H_2O$ were dissolved in separate containers with 50 mL of water each; the solutions were mixed and agitated together for 5 min, after which 3 mL of NH_4OH 25 % w/w was added dropwise at a rate of 1 mL/min. The reaction was allowed to proceed for 30 min. Then, ~25 mL of NH_4OH 25 % w/w was added until pH 10.5. NP were collected by magnetic separation, and the supernatant was discarded to remove excess ammonium. Approximately 40 mL of citric acid 0.02 g/mL was added dropwise to the NP until pH 7.4 was reached. After a second magnetic separation, the NP from the supernatant were collected (NP from the supernatant (NPs)); the precipitate was washed with 40 mL of Milli-Q water and resuspended in another 40 mL of Milli-Q water (NP from the precipitate (NPp)). All the steps were conducted at 60 °C under a nitrogen atmosphere.

Nanocomposites were prepared by reconstruction and impregnation. LDHs were calcined at 450 °C for 9 h. Then, two different Al:CBZ molar ratios were tested: 1:1 and 2:1. The drug (CBZ) was dissolved in Milli-Q water with 12 % of ethanol, and the calcined LDHs were added to the solution. The samples were agitated at 40 °C for 48 h under a nitrogen atmosphere. After that, two different washings were studied: 3 washings with Milli-Q water or 3 washings with ethanol 10 %. The composites were dried at room temperature. The names of the resulting samples are listed in Table 1. The sample with an Al:CBZ 1:1 M ratio was selected to be used in the rest of the experiments and was impregnated with the NP previously synthesized. For this, before the washing with ethanol 10 %, different amounts of NPs or NPp were added to the LDH-CBZ composites (see Table 1) and left under agitation for 24 h at 60 °C (Fig. 1).

2.3. Characterization

For drug loading measurements, a known amount of sample was placed in a 5 mL volume flask, and filled with HCl:EtOH 1:1 v:v. The concentration of CBZ (C_{CBZ}) was measured by UV/vis spectrophotometry at 285 nm, in a Jasco V-650 UV–Visible spectrophotometer. For the samples containing NP, the absorbance of Fe was subtracted with the absorbance addition method [19], where a calibration curve of CBZ and Fe must be done both at 285 nm and 241 nm (maximum absorbance of CBZ and Fe respectively) to get the molar extinction coefficient (ϵ) of each molecule at both wavelengths. The concentration of the molecules (C) can then be calculated with equations (1) and (2):

$$A_{285nm} = \varepsilon_{Fe,285nm} \times l \times C_{Fe} + \varepsilon_{CBZ,285nm} \times l \times C_{CBZ} \quad \text{Equation 1}$$

$$A_{241nm} = \varepsilon_{Fe,241nm} \times l \times C_{Fe} + \varepsilon_{CBZ,241nm} \times l \times C_{CBZ} \quad \text{Equation 2}$$

where A is the absorbance of the sample at each wavelength and l is the cuvette path length (1 cm). The amount of drug loading in the composites was calculated with equation (3) [20]:

$$\textit{Drug loading}\ (\%) = \frac{\textit{amount of drug}}{\textit{composite weight}} \times 100 \quad \text{Equation 3}$$

The X-ray diffraction patterns were taken in an X'Pert Pro-PANalytical diffractometer with Cu Kα radiation (λ = 1.54 Å), at a step time of 4.25 s and a step size of 0.026° in 2θ. Transmission electron microscopy (TEM) images were taken in a JEOL JEM EXII 1200 microscope at 80 kV, as described in Peralta et al. [9]. The diameter of the composites was also measured as described in that work,

Table 1
Design of composites and CBZ loading (% of total composite).

Sample name	Al:CBZ mol:mol	Amount of NP	Washing	Drug loading (%)
LDH-CBZ (2:1, ethanol)	2:1	0	3 with ethanol 10 %	12.4 ± 0.3
LDH-CBZ (2:1, water)	2:1	0	3 with water	33 ± 4
LDH-CBZ (1:1, ethanol)	1:1	0	3 with ethanol 10 %	48 ± 6
LDH-CBZ (1:1, water)	1:1	0	3 with water	51.1 ± 0.5
LDH-CBZ-NPp (1)	1:1	1 mL	3 with ethanol 10 %	17 ± 3
LDH-CBZ-NPp (5)	1:1	5 mL	3 with ethanol 10 %	13 ± 1
LDH-CBZ-NPp (11)	1:1	11 mL	3 with ethanol 10 %	28.5 ± 0.6
LDH-CBZ-NPs (1)	1:1	1 mL	3 with ethanol 10 %	27.4 ± 0.8
LDH-CBZ-NPs (2)	1:1	2 mL	3 with ethanol 10 %	25.9 ± 0.5
LDH-CBZ-NPs (3)	1:1	3 mL	3 with ethanol 10 %	24 ± 1

with Fiji Image J software. Surface charge of the NP was determined by ζ potential measurements with a ZetasizerNano ZS, Malvern, UK. The diameter of the crystals that form the composites (D) was measured from the X-ray patterns by the Scherrer equation [21] (Equation (4)):

$$D = \frac{k\lambda}{\beta \cos\theta} \quad \text{Equation 4}$$

where k is the Scherrer constant (0.94 for spheres and octahedrons), β is the line broadening at FWHM in radians, measured from a Gaussian fitting made in Origin Pro 2016, and θ identifies the peak at which the measurement is done.

The magnetism of the samples was evaluated in a vibrating sample magnetometer LakeShore 7300, with static field up to $\mu_0 H = 1$ T. All measurements were performed at room temperature. The magnetic properties were estimated from the magnetization loops by fitting the sum of three contributions: a ferromagnetic (Mfm), a linear paramagnetic (Mp) and a superparamagnetic-like (Msp) [22] (Equation (5)):

$$M = Msp * \left(\coth\frac{B*H}{T} - \frac{T}{BH}\right) + Mfm\frac{2}{\pi}\,atan\left(\frac{(H+Hc) * \tan\left(\frac{\pi}{2}\right) * Mr}{abs(Hc) * Mfm}\right) + Xi * H \quad \text{Equation 5}$$

where Hc, Mr, Mfm and Msp are the coercive field, remanent magnetization, the effective saturation magnetization associated with the ferromagnetic contribution, and the effective saturation magnetization of the superparamagnetic-like component of the M(H) loops. $B = \mu/k_B$, where μ is the particle magnetic moment, and k_B is the Boltzmann constant.

Drug release measurements were performed in Franz cells at 37 °C. The donor chamber was filled with the composites suspended in 1 mL of simulated body fluid (SBF, pH 7.4, prepared as in Cuello et al. [23]) or acetate buffer (pH 4.8) at a CBZ concentration of 40 μg/mL. The receptor chambers were filled with 10 mL of the same medium, and the separating membrane was of cellulose with a pore size of 14 kDa (D9527, Sigma Aldrich, USA). One mL of sample was taken from the receptors at the defined times and replaced with fresh medium. The amount of CBZ in each sample was measured by UV/Vis spectrophotometry in an Agilent Technologies Cary 60 UV–Vis® spectrophotometer, with calibration curves done in the respective media. The absorbance of Fe was corrected only in donor (initial concentration) measurements, since the NP are not able to cross the membrane.

2.4. In vitro efficacy evaluation

MDA-MB-231 or MCF-7 cells (breast cancer cells) (ATCC Manassas, VA, USA) were seeded in a 96-well plate at 10.000 cells/well in Dulbecco's Modified Eagle medium (Gibco, BRL, Invitrogen, Carlsbad, CA, USA) supplemented with 10 % fetal bovine serum (Gibco, BRL, Invitrogen, Carlsbad, CA, USA), and were incubated at 37 °C in 5 % of CO_2 under standard culture conditions; 24 h later, the medium was replaced by fresh culture medium containing the nanocomposites (dispersed in water with 2 % of DMSO). After 24 or 48 h of incubation, the cells were washed with phosphate buffered saline, and the viability was measured by MTT or Alamar Blue. Briefly, 0.1 mg of MTT or Alamar Blue 10 % dissolved in 100 μL of medium was added to each well and incubated for 4 h at 37 °C in 5 % of CO_2. In the case of Alamar Blue, samples were excited at 530 nm, and fluorescence was read at 590 nm. In the case of MTT, the supernatant was discarded, formazan crystals were dissolved with 100 μL of DMSO, and absorbance was detected at 590 nm.

Cell proliferation inhibition was calculated as depicted in equation (6) [24]:

$$Cell\ proliferation\ inhibition\ (\%) = 100 - \frac{Control\ absorbance}{Sample\ absorbance} * 100 \quad \text{Equation 6}$$

where the controls are the cells cultivated with medium without drug or composites.

2.5. Statistics

Experiments were performed in triplicate and statistics were done with unpaired t-student test with different p values. GraphPad Prism software (v. 6) was used. Results are reported as mean and standard error.

For drug release assays, the F_1 (difference, Equation (7)) and F_2 (similarity, Equation (8)) factors were calculated to evaluate the difference between the release patterns of the free drug and the samples, as described in Moore and Flanner [25]:

$$\boldsymbol{F_1 = \frac{\sum_{t=1}^{n}|Rt - Tt|}{\sum_{t=1}^{n}Rt}\, x\ 100} \quad \text{Equation 7}$$

$$\boldsymbol{F_2 = 50\ x\ log\left(\left[1 + (1/n)\sum_{t=1}^{n}(Rt - Tt)^2\right]^{-0.5}\ x\ 100\right)} \quad \text{Equation 8}$$

where Rt is the release value of the reference (pure CBZ) at the time t, Tt is the release percentage of the test (CBZ from nanocomposites) at the time t, and n is the number of time points.

F_1 factor, with values between 1 and 15, and F_2 factor between 50 and 100 indicate similarity of the curves.

3. Results and discussion

In order to decrease the problems associated with the chemotherapy of tumors, a new system composed of nanoclays of the type LDH type loaded with carbamazepine and impregnated with magnetic nanoparticles was studied.

To improve a LDH-CBZ system previously made [9], higher amounts of CBZ were added during the synthesis, and different washings were tested to eliminate the non-encapsulated drug. The X-rays diffraction patterns depicted in Fig. 2 demonstrated that all the materials presented layered double hydroxide structure with the typical planes and with d-spacings of 7.8 Å (calculated from the peak at 11.35° (003)) and well-ordered layer stacks: two defined peaks appeared at 60.7° and 62° ((110) and (113) respectively) (PCPDFWIN 70–2151). Analysis of different conditions of LDH-CBZ synthesis showed that Al:CBZ (1:1 M ratio) washed three times with water or 10 % ethanol gave the highest drug loading of 51.1 % and 48 % respectively (Table 1), with no statistical differences between them ($P = 0.59$). CBZ is soluble in ethanol and practically insoluble in water, and this is why the washing with the former is more efficient. By increasing the Al:CBZ molar ratio in the initial aqueous solution from 25:1 [9] to 1:1, the drug loading increased from 5.3 % to ~50.0 %. However, despite the washings, the X-ray diffraction patterns exhibited the typical peaks of CBZ, indicating that some drug remained in the surface layers of LDHs (Fig. 2). Anyway, the drug release patterns showed that the LDH are able to avoid the CBZ release at the blood pH (7.4) (Fig. 3B), which implies that the interaction between the layers and the drug is strong, and the CBZ is somehow protected and remains in the composite in spite of the washings, because the maximum release is not reached before 3 h. This phenomenon is better shown in the sample prepared with Al:CBZ 1:1 M ratio and washed three times with 10 % ethanol, revealing F_1 and F_2 factors of 50 and 27 respectively (Table 2), so this was the selected method for the preparation of the following composites.

On the other hand, magnetite nanoparticles were successfully synthesized. The X-ray diffraction patterns of the precipitates showed the typical peaks at $2\theta = 30.3°$, 35.5°, 43.4°, 53.7°, 57.2°, and 63.1° (Fig. 4) [26] and the magnetization curve showed a saturation magnetization of 51 emu/g and a superparamagnetic behavior (Table 3). The supernatant could not be dried, probably for an excess of citric acid, and then the X-ray diffraction patterns and magnetization curves could not be done. The NPp and the NPs diameter measured from TEM images (Fig. 5E) were similar to those reported by de Sousa et al. [15]: for NPs, 9.8 ± 0.3 and 10.9 ± 1.8 nm, for NPp, 11.9 ± 0.5 nm and 10.8 ± 2.7 nm respectively. These diameters are optimal for the proposal of this work, since they are small enough to show a superparamagnetic behavior and a high magnetization, which was also confirmed by VSM. The crystal size of NPp, measured from X-ray patterns with Scherrer equation (equation (4)), was 7.5 nm (Fig. 5E), meaning that NP are monocrystals. The ζ potential was -23.6 ± 0.4 mV and -30.6 ± 1.4 mV for NPs and NPp respectively, which also agree with those reported in the bibliography. The negative charge given by the citric acid should allow the interaction between the NP and the positive layers of the LDHs.

New syntheses of LDH-CBZ (1:1, ethanol) were then impregnated with different amounts of NPp or NPs (Table 1 lists the corresponding names of the samples). The drug loading decreased to 17 %–29 % depending on the sample, which was due to the addition of more ingredients to the samples (Table 1). In the X-ray diffraction patterns, the defined peaks at 60.7° and 62° could still be seen, which implies well-ordered layer stacks; however, in the composites impregnated with 2 and 3 mL of NPs a second d-spacing of ~11.5 Å appeared (Fig. 4 and $2\theta = 7.5°$), although the peaks corresponding to the NP did not appear. Taking into account that the addition of CBZ does not change the d-spacing of the LDHs, as was reported in Peralta et al. [9], a LDH-NPs composite was prepared, and the result was the same, meaning that the NPs exchange with the anions on the interlayers and enter into the LDHs. In the impregnations with NPp, the peaks of the NP appeared but a second d-spacing did not, which implies that the NPp were added to the surface of LDHs; this should enhance the delivery of the composites through an external magnetic field.

Fig. 5 shows some illustrative images of the composites taken by TEM, and the size of the LDHs measured from these ones. In general, the LDHs had the typical hexagonal shape. The diameter increased from 65 to 93 nm with the addition of CBZ, and to 97–120

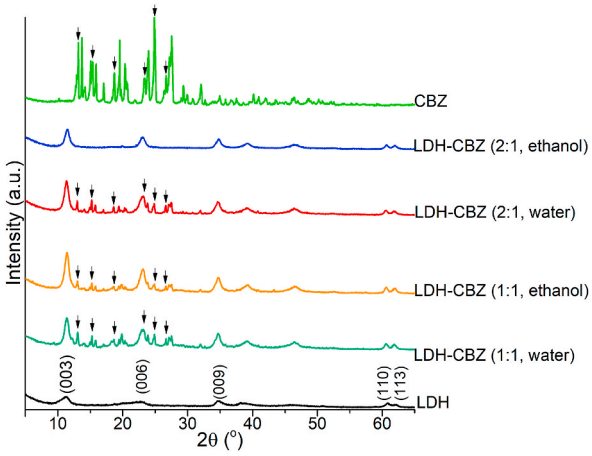

Fig. 2. X-ray diffraction patterns. The arrows indicate CBZ main peaks.

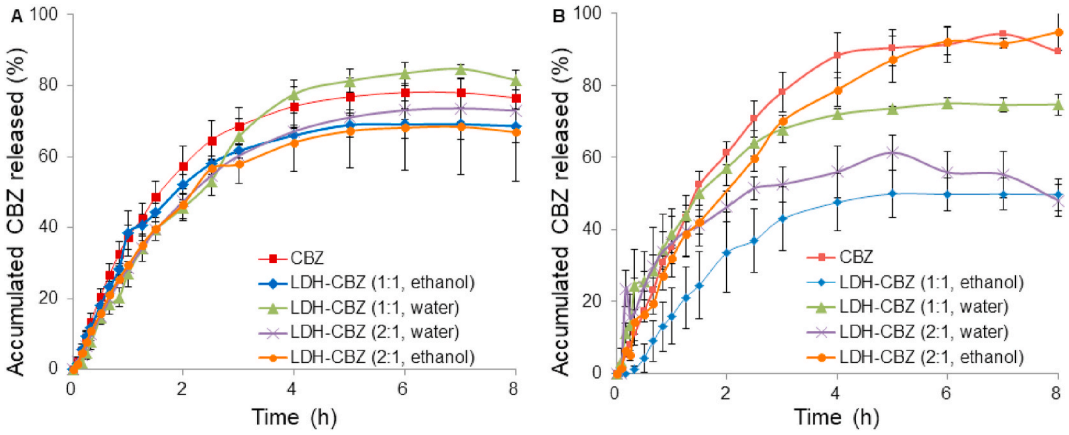

Fig. 3. Drug release profiles through A) Acetate buffer (pH 4.8) and B) SBF (pH 7.4).

Table 2
Statistics of drug release patterns. Comparisons made with respect to free CBZ. N = 3, F_1 of 0–15, and F_2 of 50–100 ensure the equality of the curves.

Sample	Medium	F_1	F_2	Result
LDH-CBZ (2:1, ethanol)	SBF	9	63	Similar curves
	Acetate buffer	16	55	Different curves
LDH-CBZ (2:1, water)	SBF	34	33	Different curves
	Acetate buffer	13	58	Similar curves
LDH-CBZ (1:1, ethanol)	SBF	50	27	Different curves
	Acetate buffer	10	63	Equal curves
LDH-CBZ (1:1, water)	SBF	17	49	Different curves
	Acetate buffer	15	56	Similar curves
LDH-CBZ-NPp (1)	SBF	20	44	Different curves
	Acetate buffer	4	79	Equal curves
LDH-CBZ-NPp (5)	SBF	24	41	Different curves
	Acetate buffer	4	79	Equal curves
LDH-CBZ-NPp (11)	SBF	23	42	Different curves
	Acetate buffer	33	40	Different curves

nm with the addition of NPp or to 142 nm with NPs (Fig. 5E). The crystals that form the composites also increased proportionally with the addition of CBZ and NPp or NPs (Fig. 5E, calculated with Scherrer equation). The NP content of each sample is related to the TEM images: it can be seen that the one with the highest content (11 mL) (Fig. 5D) presents more agglomeration than the one with the smallest content (1 mL) (Fig. 5C), in which the NPs are more dispersed. From this it can be deduced that the optimal content for a good distribution is 5 mL (Fig. 5A). The sample in Fig. 5B was synthesized with 1 mL of NP obtained from the suspension, and they are homogeneously distributed.

The magnetic measurements, shown in Fig. 6 and Table 3, revealed that all the composites were superparamagnetic. This is an important property for the pretended application since, once the external magnetic field has been removed, no magnetization remains in the composites and then in the body of the patient. The only sample that showed a little hysteresis was the LDH-CBZ-NPs (3), with a remanent magnetization of 0.26 emu/g and a coercive field of 606 Oe. Also, the magnetic saturation was higher in the samples prepared with NPp, and this is due to the magnetic separation done during the NP synthesis, which "precipitates" the most magnetic nanoparticles. In all the cases the magnetization/g was dependent on the amount of NP used during the synthesis. From TEM and VSM results, the LDH-CBZ-NPp sample was the most appropriate for the delivery of the drug to the tumors and it was selected for the rest of the experiments.

Fig. 7 shows the drug release profiles from LDH-CBZ-NPp against simulated media of different pH values. The impregnation of the nanoclays with large amount of NPp (11 mL, sample LDH-CBZ-NPp(11)) hindered the CBZ release at the cytosol pH (4.8). The amount of CBZ that passed to the receiving medium was high (60 %) but not complete. However, the impregnation with 1 and 5 mL of NPp (LDH-CBZ-NPp(1) and LDH-CBZ-NPp(5)) did not affect the release of CBZ at this pH, which was complete from the beginning: it passed from the donor to the receptor medium in the same amount as the control (free CBZ) ($F_1 = 4$ and $F_2 = 79$ in both cases, Table 2). Among the SBF (pH 7.4), all the samples gave similar results, with F_1 and F_2 factors clearly indicating a difference with respect to the control.

CBZ is a widely studied antiepileptic compound; however, its anticancer activity has been recently mentioned. A first screening was made to evaluate and confirms the antitumor activity of CBZ. Akbarzadeh et al. showed an IC50 of 5 μM in SW480 colorectal cancer cell line after two days of exposure [6]. It is worth noting that its effect could not be reproduced in this work, since higher concentrations (100–1000 μM) did not produce a cell reduction in that time (HCT 116 and SW480 cell lines were tested). On the other hand, in breast cancer cell lines, Meng et al. found ~60 % of cell inhibition with CBZ 0.1 mM in MCF-7, T-47-D and SKBR-3, and a concentration

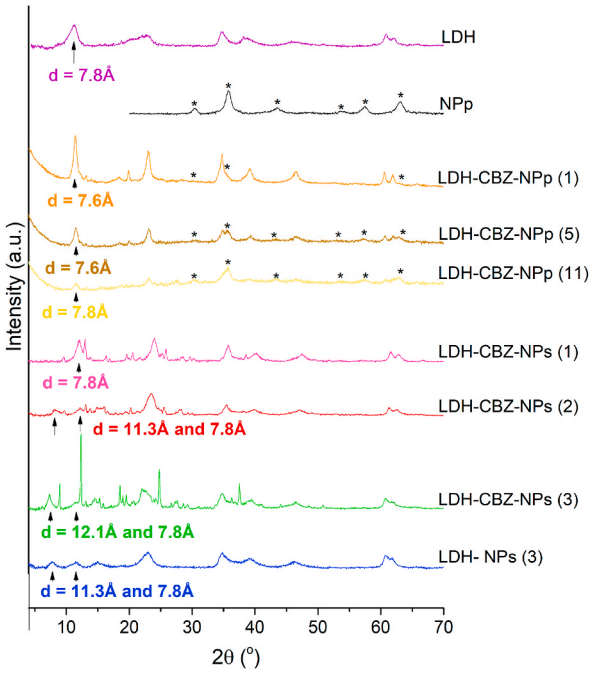

Fig. 4. X-ray diffraction patterns. The arrows indicate the peaks used to calculate each d-spacing specified in the figure. * Peaks corresponding to NP.

Table 3
Fitting of VSM measurements.

Sample	Msp	Mfm	B	X
NPp	51.0 ± 0.1	0	1.60 ± 0.02	$3.70E^{-4} \pm 8E^{-6}$
LDH-CBZ-NPp (1)	1.454 ± 0.003	0	0.821 ± 0.006	0 ± 0
LDH-CBZ-NPp (5)	9.37 ± 0.02	0	1.52 ± 0.02	$9.2E^{-5} \pm 1E^{-6}$
LDH-CBZ-NPp (11)	17.27 ± 0.02	0	1.37 ± 0.01	$1.20E^{-4} \pm 2E^{-6}$
LDH-CBZ-NPs (1)	$0.06 \pm 5E^{-5}$	0	0.671 ± 0.004	0 ± 0
LDH-CBZ-NPs (2)	0.451 ± 0.002	0	1.21 ± 0.02	$7.4E^{-6} \pm 1E^{-7}$
LDH-CBZ-NPs (3)	0.46 ± 0.05	0.74 ± 0.01	0.028 ± 0.005	0 ± 0.001

dependent behavior [5]. In this work, CBZ had a concentration dependent behavior from 0.1 to 1 mM concentrations in MCF-7 and MDA-MB-231 cell lines (Fig. 8). The highest concentration (2 mM) produced no differences with the previous one (1 mM). The compound incubation time generated little effect on all the concentrations.

Taking into account the previous results, the activity of the composites was measured by Alamar Blue in the MDA-MB-231 breast cancer cell line (Fig. 9). The incorporation of the drug in the LDH only caused an increase of the anticancer activity at 48 h and at low concentration. However, the addition of the NPp to the system significantly inhibited the growth of cancer cells. The effect was remarkable at 0.5 mM concentration, both at 24 and 48 h. The addition of different amounts of NP did not produce differences. The effect of the LDH and the NPp alone was tested at 24 h in concentrations comparable to that of the LDH-CBZ-NPp (5) 0.5 mM composite, and the cell inhibition was 0 % in both samples, which means that the materials themselves had no effect on these cells. At 1 mM concentration, the drug itself produced high activity and there were no appreciable differences with the composites.

Iron NP can be endocytosed and accumulated in the lysosomes, which can produce cytotoxicity; however, if the NP avoid the endocytosis, the cytotoxicity is not produced [27]. At least in the concentration used herein, the NPp themselves produced no effect on the breast cancer cells; de Sousa et al. did not observe antitumor activity either with citric acid coated NP in A549 cells [15]. However, when the NPp are added to the LDH-CBZ composites, the anticancer activity is significantly increased. LDHs have efficient cell membrane penetration [10,28] and they can carry the NP to the interior of the cell, producing a high accumulation and the apoptosis of the cell [3]. Komarala et al. demonstrated that Fe_3O_4 NP-LDH composites are able to penetrate the cells after 6 h of exposure and stay in the cytoplasm and the nuclei of the cells, but they do not produce any effect on murine fibroblast and human cervical cancer cells; however, they observed that the IC_{50} of doxorubicin decreased when it was encapsulated in the mentioned material [17]. These results agree with those presented herein. Then, the other option is that the system enhances the entry of CBZ to the cell and after releasing it, the drug can increase its activity.

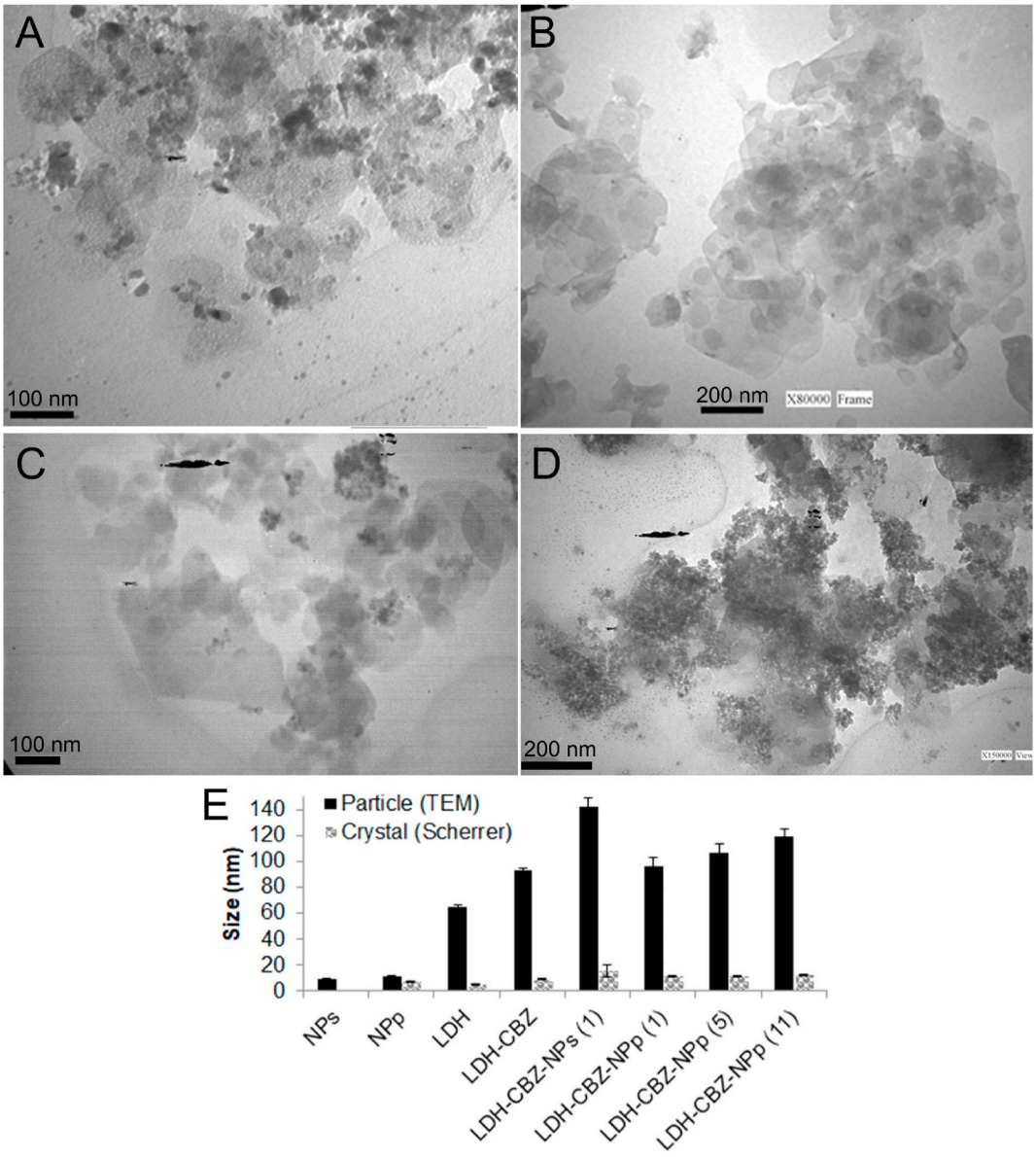

Fig. 5. TEM images of A) LDH-CBZ-NPp (5), B) LDH-CBZ-NPs (1), C) LDH-CBZ-NPp (1) and D) LDH-CBZ-NPp (11). E) Diameter of the NP, LDH and composites measured from TEM images and crystal size calculated from X-ray patterns with Scherrer equation.

4. Conclusion

All the composites assayed were well synthesized: they presented a layered double hydroxide form and could be loaded with CBZ. From the different systems, that impregnated with 5 mL of precipitated iron nanoparticles achieved 12 % of drug loading, which was enough to enhance the efficacy of carbamazepine against breast cancer cells from 62 % to 92 %. Moreover, the saturated magnetization obtained was high without the need of using large amounts of nanoparticles and should be adequate to attract the material with an external magnetic field located near the tumor site; also, the material showed a superparamagnetic behavior that avoids the remanent magnetization of the body after removing the external magnetic field. The diameter of the compounds remained nanometric (106 nm), which is good for systemic drug delivery, and the release at different pH values was efficient: the nanoclay slowed down the CBZ release at the blood pH and released it faster at the pH of the lysosomes. The resultant system is promising and *in* vivo experiments are required to analyze the nanocomposite delivery to the tumors through an external magnetic field and its efficacy.

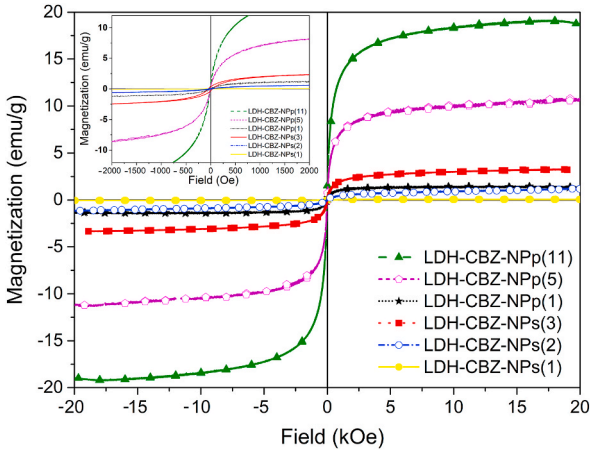

Fig. 6. VSM measurements. The inset shows a magnification to see the hysteresis loop of the LDH-CBZ-NPs(3) sample.

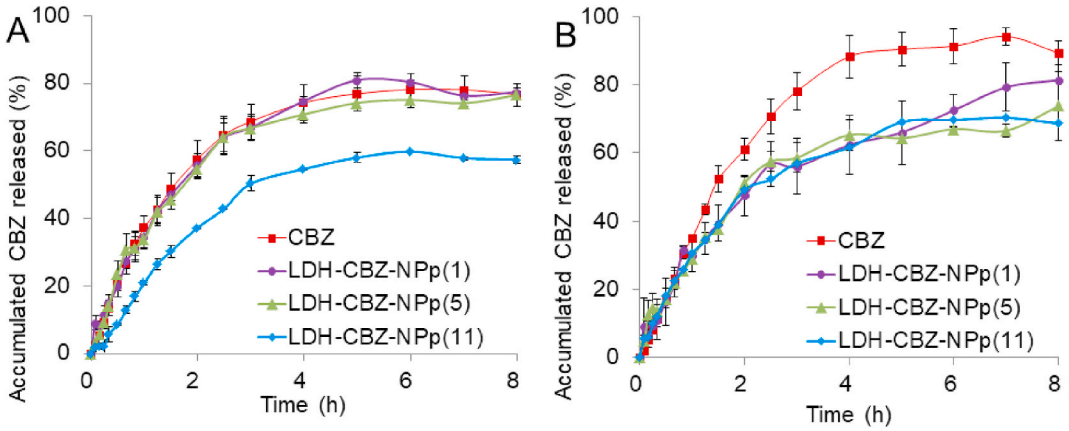

Fig. 7. Drug release profiles through A) Acetate buffer (pH 4.8) and B) SBF (pH 7.4).

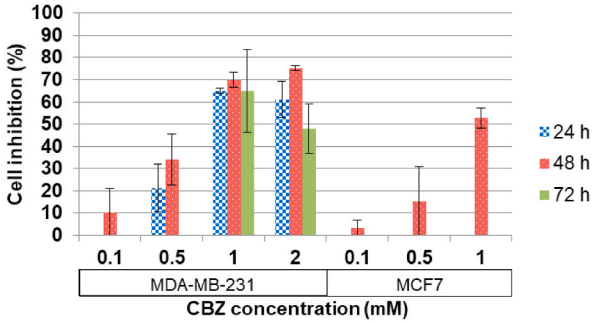

Fig. 8. Breast cancer cell proliferation inhibition measured by MTT, calculated with respect to the control without treatment.

Funding

This research was funded by Secretaría de Ciencia y Tecnología – Universidad Nacional de Córdoba (SeCyT 2018–2021, Res. 266/18) and from CONICET (PIP 2021–2023) to GEG; from Agencia Nacional de Promoción de la Investigación, el Desarrollo Tecnológico y la Innovación (PICT 2018–02367) and from Universidad Tecnológica Nacional (SCyT-UTN 2021–2023) to MEC; from Universidad Tecnológica Nacional (SCyT-UTN 2020–2022) to SNM. The funding sources had no role in the study design, collection, analysis and interpretation of data, in the writing of the report, or in the decision to submit the article for publication.

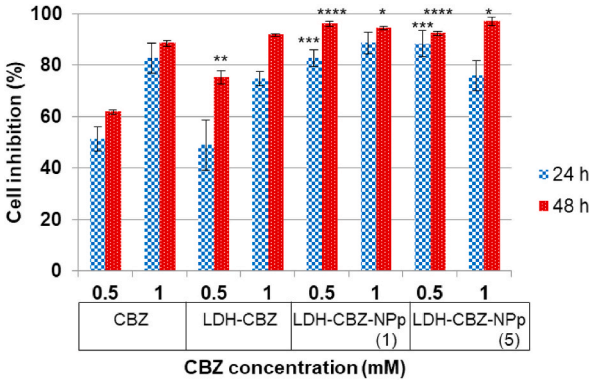

Fig. 9. MDA-MB-231 breast cancer cell proliferation inhibition by CBZ, measured by Alamar Blue, calculated with respect to the control without treatment. *P ≤ 0.01 **P ≤ 0.009 ***P ≤ 0.0003 ****P ≤ 0.0001 compared to free drug (CBZ 0.5 and 1 mM).

Data availability statement

Data associated with the study have not been deposited into a publicly available repository because they have been included in the article.

CRediT authorship contribution statement

M. Florencia Peralta: Conceptualization, Methodology, Writing – original draft. **Silvia N. Mendieta:** Conceptualization, Funding acquisition, Writing – review & editing. **I. Romina Scolari:** Methodology, Writing – review & editing. **M. Verónica Gerbaldo:** Methodology, Writing – review & editing. **Marcos I. Oliva:** Methodology, Writing – review & editing. **Germán A. Gil:** Funding acquisition, Writing – review & editing. **Gladys E. Granero:** Funding acquisition, Writing – review & editing. **Mónica E. Crivello:** Conceptualization, Funding acquisition, Writing – review & editing.

Declaration of competing interest

The authors declare that they have no known competing financial interests or personal relationships that could have appeared to influence the work reported in this paper.

Acknowledgements

The authors would like to thank Consejo Nacional de Investigaciones Científicas y Técnicas (CONICET), Universidad Tecnológica Nacional (UTN) and Universidad Nacional de Córdoba (UNC) for their financial support. They would also like to thank the X-ray Diffraction Laboratory, from Instituto de Investigaciones en Fisicoquímica de Córdoba-CONICET-UNC.

References

[1] Cancer today. International Agency for Research on Cancer 2023, (2020). https://gco.iarc.fr/today/online-analysis-multi-bars?v=2020&mode=cancer&mode_population=countries&population=900&populations=900&key=asr&sex=0&cancer=39&type=0&statistic=5&prevalence=0&population_group=0&ages_group%5B%5D=0&ages_group%5B%5D=17&nb_items=10& (accessed January 12, 2023).
[2] R.L. Siegel, K.D. Miller, H.E. Fuchs, A. Jemal, Cancer statistics, 2022, CA, Cancer J. Clin. 72 (2022) 7–33, https://doi.org/10.3322/caac.21708.
[3] A.K. Gupta, M. Gupta, Synthesis and surface engineering of iron oxide nanoparticles for biomedical applications, Biomaterials 26 (2005) 3995–4021, https://doi.org/10.1016/j.biomaterials.2004.10.012.
[4] Q. Meng, X. Chen, L. Sun, C. Zhao, G. Sui, L. Cai, Carbamazepine promotes Her-2 protein degradation in breast cancer cells by modulating HDAC6 activity and acetylation of Hsp 90, Mol. Cell. Biochem. 348 (2011) 165–171, https://doi.org/10.1007/s11010-010-0651-y.
[5] Q.-W. Meng, C.-H. Zhao, Y.-H. Xi, L. Cai, L.-C. Sun, G.-J. Sui, Inhibitory effect of carbamazepine on proliferation of estrogen-dependent breast cancer cells, Ai zheng = Chinese, J. Cancer 25 (2006) 967–973.
[6] L. Akbarzadeh, T. Moini Zanjani, M. Sabetkasaei, Comparison of anticancer effects of carbamazepine and valproic acid, Iran, Red Crescent Med. J. 18 (2016), https://doi.org/10.5812/ircmj.37230.
[7] A.L.M.D. de Sousa, W.M. dos Santos, M.L. de Souza, L.C.P.B.B. Silva, A.E.H.K. Yun, C.S.B. Aguilera, B. de F. Chagas, L.A. Rolim, R.M.F. da Silva, P.J.R. Neto, Layered double hydroxides as promising excipients for drug delivery purposes, Eur. J. Pharmaceut. Sci. 165 (2021), 105922, https://doi.org/10.1016/j.ejps.2021.105922.
[8] C. Prasad, H. Tang, W. Liu, Magnetic Fe3O4 based layered double hydroxides (LDHs) nanocomposites (Fe3O4/LDHs): recent review of progress in synthesis, properties and applications, J. Nanostructure Chem. 8 (2018) 393–412, https://doi.org/10.1007/s40097-018-0289-y.
[9] M.F. Peralta, S.N. Mendieta, I.R. Scolari, G.E. Granero, M.E. Crivello, Synthesis and release behavior of layered double hydroxides – carbamazepine composites, Sci. Rep. (2021), https://doi.org/10.1038/s41598-021-00117-9.
[10] G. Mishra, B. Dash, S. Pandey, Layered double hydroxides: a brief review from fundamentals to application as evolving biomaterials, Appl. Clay Sci. 153 (2018) 172–186, https://doi.org/10.1016/j.clay.2017.12.021.
[11] M. Ebadi, K. Buskaran, S. Bullo, M.Z. Hussein, S. Fakurazi, G. Pastorin, Drug delivery system based on magnetic iron oxide nanoparticles coated with (polyvinyl alcohol-zinc/aluminium-layered double hydroxide-sorafenib), Alex. Eng. J. 60 (2021) 733–747, https://doi.org/10.1016/j.aej.2020.09.061.

[12] V. Ambrogi, F. Marmottini, C. Pagano, Amorphous carbamazepine stabilization by the mesoporous silicate SBA-15, Microporous Mesoporous Mater. 177 (2013) 1–7, https://doi.org/10.1016/j.micromeso.2013.04.008.
[13] A. Donnadio, C. Corneli, P. Ricci, M. Bini, V. Ambrogi, Use of calcium carbonate as an excipient for release of poorly water soluble drugs: the case of carbamazepine, Int. J. Pharm. 589 (2020), 119860, https://doi.org/10.1016/j.ijpharm.2020.119860.
[14] X. Yang, X. Zhang, Y. Ma, Y. Huang, Y. Wang, Y. Chen, Superparamagnetic graphene oxide–Fe3O4nanoparticles hybrid for controlled targeted drug carriers, J. Mater. Chem. 19 (2009) 2710–2714, https://doi.org/10.1039/B821416F.
[15] M.E. de Sousa, M.B. Fernández van Raap, P.C. Rivas, P. Mendoza Zélis, P. Girardin, G.A. Pasquevich, J.L. Alessandrini, D. Muraca, F.H. Sánchez, Stability and relaxation mechanisms of citric acid coated magnetite nanoparticles for magnetic hyperthermia, J. Phys. Chem. C 117 (2013) 5436–5445, https://doi.org/10.1021/jp311556b.
[16] X.-F. Zhao, W.-Y. Wang, X.-D. Li, S.-P. Li, F.-G. Song, Core-shell structure of Fe3O4@MTX-LDH/Au NPs for cancer therapy, Mater. Sci. Eng. C. 89 (2018) 422–428, https://doi.org/10.1016/j.msec.2018.04.024.
[17] E.P. Komarala, S. Nigam, M. Aslam, D. Bahadur, In-vitro evaluation of layered double hydroxide–Fe3O4 magnetic nanohybrids for thermo-chemotherapy, New J. Chem. 40 (2016) 423–433, https://doi.org/10.1039/C5NJ01701G.
[18] S. Barkhordari, A. Alizadeh, Fabrication of pH-sensitive chitosan/layered double hydroxide (LDH)/Fe3O4 nanocomposite hydrogel beads for controlled release of diclofenac, Polym. Bull. 79 (2022) 5533–5548, https://doi.org/10.1007/s00289-021-03761-3.
[19] Cuantificación de dos analitos con UV vis empleando el método de adición de absorbancias,(n.d.). https://quimicafacil.net/manual-de-laboratorio/adicion-de-absorbancias/(accessed January 12, 2023)..
[20] S. Mokhtari, M. Solati-Hashjin, Z. Khosrowpour, M. Gholipourmalekabadi, Layered double hydroxide-galactose as an excellent nanocarrier for targeted delivery of curcumin to hepatocellular carcinoma cells, Appl. Clay Sci. 200 (2021), 105891, https://doi.org/10.1016/j.clay.2020.105891.
[21] M.R. Arefi-Rad, H. Kafashan, Pb-doped SnS nano-powders: comprehensive physical characterizations, Opt. Mater. 105 (2020), 109887, https://doi.org/10.1016/j.optmat.2020.109887.
[22] M.B. Stearns, Y. Cheng, Determination of para- and ferromagnetic components of magnetization and magnetoresistance of granular Co/Ag films (invited), J. Appl. Phys. 75 (1994) 6894–6899, https://doi.org/10.1063/1.356773.
[23] N.I. Cuello, V.R. Elías, S.N. Mendieta, M. Longhi, M.E. Crivello, M.I. Oliva, G.A. Eimer, Drug release profiles of modified MCM-41 with superparamagnetic behavior correlated with the employed synthesis method, Mater. Sci. Eng. C. 78 (2017) 674–681, https://doi.org/10.1016/j.msec.2017.02.010.
[24] M.F. Peralta, M.E. Bracamonte, M.L. Guzman, M.E. Olivera, J.D. Marco, D.C. Carrer, P.A. Barroso, Efficacy of topical miltefosine formulations in an experimental model of cutaneous leishmaniasis, Drug Deliv. Transl. Res. 12 (2021) 180–196, https://doi.org/10.1007/s13346-021-00896-8.
[25] J.W. Moore, H.H. Flanner, Mathematical comparison of dissolution profiles, Pharmaceut. Technol. 20 (1996) 64–74.
[26] M.R. Alibeigi, Samaneh, Vaezi, Phase transformation of iron oxide nanoparticles by varying the molar ratio of Fe2+:Fe3+, Chem. Eng. Technol. 31 (2008) 1591–1596, https://doi.org/10.1002/ceat.200800093.
[27] D. Guarnieri, S. Sabella, O. Muscetti, V. Belli, M.A. Malvindi, S. Fusco, E. De Luca, P.P. Pompa, P.A. Netti, Transport across the cell-membrane dictates nanoparticle fate and toxicity: a new paradigm in nanotoxicology, Nanoscale 6 (2014) 10264–10273, https://doi.org/10.1039/C4NR02008A.
[28] S. Senapati, R. Thakur, S.P. Verma, S. Duggal, D.P. Mishra, P. Das, T. Shripathi, M. Kumar, D. Rana, P. Maiti, Layered double hydroxides as effective carrier for anticancer drugs and tailoring of release rate through interlayer anions, J. Contr. Release 224 (2016) 186–198, https://doi.org/10.1016/j.jconrel.2016.01.016.